Published in final edited form as:
Nat Neurosci. 2014 March ; 17(3): 463–470. doi:10.1038/nn.3649.

A neural mechanism underlying failure of optimal choice with multiple alternatives

Bolton KH Chau[1,*], **Nils Kolling**[1], **Laurence T Hunt**[2], **Mark E Walton**[1], and **Matthew FS Rushworth**[1,2]

[1]Department of Experimental Psychology, University of Oxford, South Parks Road, Oxford OX1 3UD

[2]FMRIB Centre, University of Oxford, John Radcliffe Hospital, Oxford OX3 9DU

Abstract

Despite widespread interest in neural mechanisms of decision-making most investigations focus on decisions between just two options. Here we adapt a biophysically plausible model of decision-making to predict how a key decision variable–the value difference signal–encoding how much better one choice is than another, changes with the value of a third, but unavailable, alternative. The model predicts surprising failures of optimal decision-making – greater difficulty choosing between two options in the presence of a third very poor, as opposed to very good, alternative. The prediction was borne out, first, by investigation of human decision-making and, second, functional magnetic resonance imaging-(fMRI)-based measurements of value difference signals in ventromedial prefrontal cortex (vmPFC); the vmPFC signal decreased in the presence of low value third alternatives and vmPFC effect sizes predicted individual variation in sub-optimal decision-making in the presence of multiple alternatives. The effect contrasts with that of divisive normalization in parietal cortex.

Introduction

Despite the ubiquity of value representations in the brain[1], but there is special interest in vmPFC and intraparietal sulcus (IPS) because several lines of evidence suggest they use value information to guide a decision process[2-6]. Not only do these areas carry information about reward expectation[3,7-15], but vmPFC, and sometimes IPS, also carry "value difference" signals reflecting the difference in value between chosen and unchosen options during decision-making in a way that suggests value comparison between options is taking place[3,5,9,16-19].

Despite broad interest in the neural mechanisms of decision-making, little is known about the comparison process when there are multiple, and not simply two, alternatives to choose between. One important study of visually-guided decisions (evidence accumulation

[*]Corresponding author. Phone: (+44) 1865 271309; boltonchau@gmail.com.
Author contributions: experimental design: BKHC, MEW, & MFSR; behavioral and MRI data collection and analysis: BKHC; biophysical modelling: NK & LH; manuscript preparation: BKHC & MFSR.

We declare no competing financial interests.

Europe PMC Funders Author Manuscripts

processes in value-guided and visually-guided decisions share many features[3,17,20,21]) explicitly compared multi-alternative and binary visual decisions but the degree of evidence for only one of the two/four possible choices was manipulated on each trial[22]. By contrast, in the present study, we investigate decisions where the value related to each of several potential options is parametrically varied on each decision so that the interactions between neural representations of several potential choices can be investigated.

There are four parts to the investigation. First, we extend a biophysical model of decision-making by *competition through mutual inhibition*[23,24] to predict how the value difference signal for two options changes as a function of the value of a third distracting alternative that cannot itself be selected. We then compared model predictions with human choices and neural activity in vmPFC and the medial IPS region (MIP). Human MIP corresponds to macaque MIP[25] and is concerned with value-guided decisions[3,25] and evidence accumulation[26] when choices are made with the hands. Finally, we explored the relationship between our findings and the influential *divisive normalization* model of multi-alternative decision-making[27].

Results

Biophysical model of multiple option decision-making

We extended a biophysical cortical attractor network model[24] for making decisions between two options which has previously predicted value difference signals in vmPFC and IPS when there are two choices[3,28]. Our model was similar but included three rather than two populations of excitatory pyramidal neurons that represented potential choices (Fig.1a). Each population's neurons received an input proportional to the value of one option. Just as in the original model, there was strong recurrent excitation between neurons *within* populations but interneuron-mediated inhibition *between* populations. The inhibition between populations instantiates a competition that leads to an attractor state in which one single population has a high firing rate, and the others low firing rates; the corresponding option is thus 'chosen' by the network. High value options are more likely to be chosen by the network because their representative population receives stronger external excitatory input.

We examined how the comparison between two options was affected by the presence of a third alternative in a manner that would generate predictions of behavior and brain activity. Obviously, if the third alternative has the highest value, then it might itself be selected. In those cases behavior will be silent as to how the first two options were compared. If the third option is always lowest in value then it will have little parametric range and its value is easily confounded with those of the first two options. We therefore examined the impact of a third option that might be considered a transitorily available "distractor" – an option with a potential value but which could not itself be chosen. To ensure that it could briefly be considered a potential alternative, the identity of the distractor was only revealed shortly after (100ms) all three options were presented. Therefore, initially, all three populations of neurons, representing the high and low value available options (P_{HV}, P_{LV} respectively; figure 1a) and the distractor (P_D;Fig.1a) become active and inhibit one another indirectly through an inhibitory population (P_I; Fig.1a). The distractor option input was removed 100

ms after presentation and the inputs for the other two choosable options were switched off 800ms after presentation (Online Methods). We sampled the activity of P_{HV} and P_{LV} in the period 700-1200 ms after presentation to estimate which option would be most active, and therefore likely to be chosen, in a speeded reaction time (RT) decision. Model parameters were selected such that the frequency of choices between the two available options reflected subjects' performance in the task described below (fig 1b).

From here on we refer to the values of the two available options the model could select as high value (HV) and low value (LV) options, and to the third option as the distractor (D). We show that what should be an irrelevant value difference, HV−D (Online Methods), has an impact on the size of the signal representing the key value difference for decision-making – HV−LV – in the biophysical model, human behavior, and brain activity.

We focused (Fig.1c, Supplementary Information SI.1) on the difference in P_{HV} and P_{LV} population activity levels because it: 1) is the key decision variable determining likelihood of HV being chosen – an accurate choice of HV is more likely when the P_{HV}-P_{LV} difference is large; 2) may correspond to the HV−LV value difference signal recorded from vmPFC when decisions are made correctly[3,5,9,16-19,29]. We look for this signal and the irrelevant value difference HV−D in the last part of our investigation and so we ensured HV−LV and HV−D shared less than 25% of their variance in the set of options we gave the network. Signals with similar levels of shared variance are separable in fMRI data[9].

We carried out our test by regressing the P_{HV}-P_{LV} population activity difference onto HV −D – the irrelevant relative difference in value between an available option and distractor – and found a *negative* relationship even when the regression model included other factors (HV−LV and HV+LV, SI.1); P_{HV}-P_{LV} population difference, the signal in favor of optimal choice, decreased as distractor value decreased (i.e. HV−D increased). The effect was even more prominent in trials when HV−LV was small (Fig.1c). We examined HV−D because, like HV−LV, it is a value difference and so it is feasible to look for a corresponding value difference signal in brain activity in later parts of the investigation. It is, of course, possible to carry out the analysis by regressing P_{HV}-P_{LV} onto the absolute distractor value – D (SI.2) – but the inference remains the same: the P_{HV}-P_{LV} signal difference decreased as distractor value decreased. To see how the effect emerges, the average P_{HV}-P_{LV} firing activities at two different values of D are also shown (Fig.1.d).

The reason for the effect became apparent when inhibitory interneuron activity was regressed onto HV−D (Fig.1e); there was less inhibitory interneuron activity when HV−D was higher (the relative value of D was lower). In other words, low value distractors lead to *less* inhibition between populations, which in turn lead to P_{LV} population activity being closer to, and sometimes exceeding, P_{HV} population activity during the time period when network activity first makes non-random decisions (SI.2). This will sometimes lead to LV rather than HV being chosen when the relative value of D is lower. When there is increased inhibition, it has a bigger impact on P_{LV} because it is more likely to ensure P_{LV}'s activation level falls to a point where it can no longer exert any competitive effect against P_{HV}. It is also noted that the effect of HV−D on inhibitory activity changed from negative to positive after 800 ms. Since the competition was resolved more quickly with larger initial inhibitory

activity in cases when D was large, the overall activities of P_{HV} and P_{LV} also dropped earlier in the trial, which in turn resulted in a smaller input to the inhibitory population at the end of the trial.

Such regression analyses of model activity can be linked to the regression analyses of fMRI data we report below. However, to predict human choice behavior we looked at the impact of D on which choice the model made – in other words we examined whether D had an impact on whether P_{HV} or P_{LV} entered the higher firing attractor model state. After an initial rise in both populations' activity the model entered stable attractor states (Fig.1f). The initial rise in both populations is a consequence of the relatively high input scaling employed to best simulate human choice behavior (Fig.1b). It is consistent with the observation that activity in neural circuits for decision-making initially reflects the sum of choice values prior to reflecting value difference[3]. Analysis of attractor states revealed the model was more likely to make an erroneous LV choice when D was much lower in value than the choosable options (Fig.1g).

By examining the impact of transient value information that does not relate to a choosable option, we have devised the most challenging, and arguably most ecologically valid, test of distractor value impact on decision-making; if even transitorily available value information can disrupt the way in which a decision is made then the phenomenon we are investigating may be a prevalent one. However, we report an additional model simulation in Supplemental Modeling demonstrating that both model and behavioral effects, remain robust even when the distractor is a third choosable option. Obviously in this situation D must be lower in value than both HV and LV (or else D itself might be chosen).

Human multiple option decision-making

We designed a task to test the model's predictions regarding the impact of an additional distracting alternative on decision-making. Participants made decisions between two options under two conditions on interleaved trials.

On two-option trials, participants saw two visual stimuli, choosing one with a spatially congruent keypad response (Fig.2). Their values corresponded to those used when testing the model in the first part of the investigation. On distractor trials, three options were presented. However, one of the options was indicated as a distractor 100ms after presentation so that decisions could only be made between the other two available options (Fig.2a). This allowed examination of how decisions were made between two options as a function of their difference in value (HV−LV), just as in the two-option trials, but now, in addition, we could also test how that comparison process was influenced by the presence of another alternative (D) that also varied in value. As with the biophysical model, by requiring participants to reject the distractor we could examine the impact of the full parametric range of alternative third values on HV−LV value comparison and decorrelated the third value, D (and HV−D), from HV and LV, HV−LV. Each distractor trial had a matched two-option trial with identical reward probabilities and magnitudes for the two available options. Any behavioral effects found only on distractor trials must therefore be due to distractor presence.

We investigated the effect of distractor value on decision-making by performing a logistic regression analysis. We included value differences between the available options (HV−LV), their sum (HV+LV) and value difference between the higher value option and the distractor (HV−D) as regressors, plus an interaction regressor (HV−LV)(HV−D). Another regressor indexed two-option or distractor trial type.

Not surprisingly, subjects made more mistakes as HV−LV decreased (β=0.554, t_{20}=13.737, p<0.001) but intriguingly the same was true when HV−D was large (β=−0.179, t_{20}=−2.292, p=0.033; Fig.2c), suggesting it was more difficult to choose HV when the distractor had a much lower value. Finally, the interaction term (HV−LV)(HV−D) was also significant (β=0.279, t_{20}=3.466, p=0.002), showing that the effect of HV−D causing inaccurate decisions diminished when HV−LV was larger. Subjects were less accurate in distractor than two-option trials (β=−0.081, t_{20}=−2.455, p=0.023). In SI.3 we show that the HV−D effect was only present on distractor and not on two-option trials. SI.4 and SI.5 present complementary analyses and alternative regression models of both human behavior and of biophysical model activity. In summary, although the distractor's impact on accuracy might seem surprising, it is consistent with the predictions of the biophysical model (Fig.1g). These behavioral data were collected during fMRI scanning in the experiment reported below but effects were robust and replicated under a number of additional conditions (SI. 6-8).

Impact of distractor value on neural signals of value

We next investigated whether distractor value impacted on neural signals for decision-making and whether this could explain accuracy decrements when the distractor value was low. There is a vmPFC blood oxygen level dependent (BOLD) "value difference signal" (HV−LV) when subjects choose correctly[3,5,9,16-19]. The first analysis therefore looked for regions where BOLD was positively correlated with HV−LV in both correctly performed two-option and distractor trials. It identified a similar vmPFC region to that seen in previous studies (Fig.3a).

The time course of the vmPFC HV−LV value difference signal in distractor trials was extracted at coordinates from previous studies[5,18] (Fig.3c) and used in analyses with orthogonal contrasts. We also extracted the HV−LV signal in the MIP region of interest (ROI) [25] (Fig.3b,d). The biophysical model predicted HV−LV value difference signals should be attenuated with low distractor values, so we tested whether the same was true in the brain. We divided the distractor trials into four bins according to HV−D and plotted peak HV−LV effect size in each bin (Fig.4a) and tested whether there was a consistent decrease in peak effect size across subjects as HV−D increased (consistent negative slope for each individual's best fitted line in Fig.4a). Consistent with model prediction, vmPFC HV−LV value difference signals were weaker when distractor values were smaller (i.e. HV−D was larger; average slope: β=−0.065, t_{20}=−3.200, p=0.005; Fig.4a).

To demonstrate that change in HV−LV signal across bins was really due to changing distractor values rather than some confound in our design, we also binned the matched two-option trials in an identical manner. It was therefore possible to examine HV−LV signals in two-option trials as a function of the absent distractor value that would have been present on

its matched distractor trial (Fig.4c). As an additional precaution, we only analyzed trials performed correctly in both two-option and distractor trial conditions. This ensured that any HV−LV signal modulation differences between conditions could not be attributed to differences in choices (biophysical model effects remained present even when analysis was restricted to correctly performed difficult trials: SI.9). Note that, just as it cannot predict other aspects of behavioral change between two and three choice situations, the model cannot predict the relative heights of the lines in figures 4a and 4c (without knowledge of how neurons are assigned to different options) but it does predict that only the line in 4a should be sloped and this is what we found. There was no significant effect of the absent "distractor" on two-option trials (β=0.010, t_{20}=0.451, p=0.657; Fig.4c); and effects in two-option and distractor conditions differed significantly (t_{20}=2.211, p=0.039). HV−LV signal weakening in vmPFC in distractor trials is a consequence of distractor presence.

Notably, the impact of distractor values on HV−LV signals in MIP did not reach significance on either distractor (β=−0.032, t_{20}=−1.271, p=0.218; Fig. 4b) or two-option trials (β=−0.034, t_{20}=−1.121, p=0.276; Fig.4d), nor was there any difference between conditions (t_{20}=−1.230, p=0.233). An ANOVA comparing change in HV−LV signals in MIP and vmPFC in two-option and distractor conditions confirmed a significant interaction ($F_{1,20}$=6.104, p=0.023). In additional control analyses, we also showed that the effect of HV −D on vmPFC signal was neither driven by variance in HV nor HV+LV (SI.10). Our results suggest that distractor impact on accuracy might be mediated via vmPFC rather than parietal cortex.

To test this possibility we looked at vmPFC value difference signals in a complementary way, instead of binning HV−LV signals by HV−D, we carried out an analysis of vmPFC BOLD looking at the interaction term (HV−LV)(HV−D) (Fig.5a). A key strategy to achieve high accuracy in distractor trials is to focus on the most relevant value comparison – that between the available options (HV−LV). Incorporating the irrelevant HV−D information into this comparison could result in less accurate representation of the value difference and this may lead to suboptimal decisions. We examined individual differences in average accuracies in distractor trials to see if they were related to individual differences in the vmPFC (HV−LV)(HV−D) signal by a partial correlation analysis, with RT and other neural signals as controlling factors. Individuals with lower accuracies had more negative (HV −LV)(HV−D) signals (r=0.512, p=0.030; Fig.5b). The relationship between the (HV−LV) (HV−D) signal and inaccurate behavior was especially strong at late time periods suggesting prolonged (HV−LV)(HV−D) modulation of vmPFC BOLD led to suboptimal decisions. To further test this hypothesis, we extracted this signal from an earlier period and calculated how much the signal size changed. Individuals that showed stronger *reduction* of the negative (HV−LV)(HV−D) signal had higher accuracies (r=0.607, p=0.008; Fig.5c).

Psychophysiological interactions of vmPFC

So far we have referred to vmPFC as a decision-maker but an alternative account emphasizes its role in attentional selection[2,30]. The finding that variation in accuracy is related to variation in vmPFC (HV−LV)(HV−D) signal is consistent with a variant of the latter hypothesis in which vmPFC does not just compare values of potential choices but

selects key choices that might be compared as opposed to irrelevant distracting, albeit value-laden, information in the environment.

We looked for further evidence for whether vmPFC might, respectively, facilitate or suppress representation of information relevant or irrelevant for the value comparison at hand. We carried out a psychophysiological interaction (PPI) analysis of all trial data seeking brain regions in which BOLD changed its coupling with vmPFC as a function of the irrelevant value contrast (HV−D). We found a large swathe of lateral orbitofrontal cortex (lOFC) extending into ventrolateral prefrontal cortex to be negatively coupled with vmPFC as a function of HV−D (cluster-forming threshold $z>2.3$, $p<0.05$ cluster-corrected, Fig.6a). Unlike vmPFC, lOFC is less important for value comparison but instead lesion, single neuron recording, and fMRI studies[2,9,10,31-33] suggest it represents precise associations between stimuli and specific outcomes. Here, we extend this to suggest that the relevance of the stimulus-reward representation encoded in lOFC may affect its coupling with vmPFC. A second part of the PPI analysis, focusing on the same lOFC region, found an area of positive coupling with vmPFC as a function of the relevant value comparison, HV−LV (cluster-forming threshold $z>2.7$, $p<0.05$ cluster-corrected, Fig.6b).

Causality cannot be inferred from PPI analysis, and it is unclear whether the results reflect an increased influence of vmPFC over lOFC, or vice versa. The former interpretation is consistent with an otherwise surprising finding[2] that lesions in this vicinity sometimes cause macaques to become worse at choosing as the difference in value between two better options and a third, lower value item increases[2] whereas normally such differences make decision-making easier. Such a deficit might be expected if vmPFC lesions prevented focusing on the most relevant comparisons when making decisions. Other lesion findings might be interpreted in a related manner[34].

Divisive normalization of spatial value signals in MIP

Our demonstration that (i) decision-making accuracy and (ii) vmPFC value difference signals are reduced in the presence of low value distractors seems at odds with an influential account of multi-alternative decision-making[27]. It argues that divisive normalization, a standard form of gain control operating in sensory systems and which may explain attentional modulation in sensory systems[35,36], also impacts on choice valuation. According to this account, value signals are diminished by *high*, rather than low, value distractors. For example, IPS neuron activity is correlated with the value of saccades to targets in their receptive fields but the activity is normalized by values of alternative targets outside the receptive field[27]; the activity associated with a target is *reduced* by a greater amount if there is a *high* value alternative elsewhere in the visual field than if there is a low value alternative.

It is, however, important to remember that divisive normalization is prominent in sensorimotor areas. Typically neurons exhibiting divisive normalization, like those in IPS, have spatially-specific receptive fields and there is evidence that IPS selects spatial locations for behavioral priority[37]. By contrast, range normalization when reported in prefrontal cortex appears on the timescale of sessions, and to a lesser extent on individual trials[38]. It is

therefore possible that trial-to-trial divisive normalization in parietal cortex might be apparent if we look for *spatially-selective* value signals.

In the next analysis, rather than looking for activity covarying with the chosen option's value irrespective of its spatial position, as we had done up to now, we looked for activity covarying with the value of choices made to a particular side of space[39]. We focus here on MIP and vmPFC signals covarying with values of correct choices made with the *contralateral* hand. We tested whether such contralateral option (COpt) choice signals were diminished when the *total value* of the options associated with the *ipsilateral* response (ipsilateral value: IV) was higher. Consistent with divisive normalization accounts[15] the MIP COpt signal was significantly diminished as IV increased (β=−0.053, t_{20}=−3.490, p=0.002; Fig.7b). No such effect, however, was seen in vmPFC (β=0.015, t_{20}=0.684, p=0.502; Fig.7a).

We also found that RTs varied in the manner predicted by a divisive normalization account. RTs increased as IV increased (β=0.142, t_{20}=3.240, p=0.004; in other words subjects were slower when the total value of options was larger in the hemifield opposite to the COpt), whereas RTs were unaffected by values of unchosen options or distractor when they were on the same side of the COpt (β=−0.028, t_{20}=−0.450, p=0.658). Next, we therefore investigated whether individual variation in RT was related to individual variation in the divisive normalization of MIP COpt signals. This also provides a way of testing whether MIP activity is actually related to task performance. We first estimated the impact of distractor value on the COpt signal in each subject by looking at the COpt×IV interaction. As expected, the interaction term was associated with a negative modulation of the BOLD signal suggesting that IV diminished the COpt signals (Fig.7c). Across subjects variation in the COpt×IV interaction term was negatively correlated with RT (r=−0.485, n=21, p=0.042; Fig.7d) after controlling for accuracy and other neural signals.

Discussion

We showed that a biophysical model of decision-making through mutual inhibition, predicts that a key decision variable, the signal encoding the difference in value between two choices, is *reduced* in the presence of a low value alternative because it imposes only weak inhibition on both better and worse potential choices, leaving them both relatively active. Both value difference signals in vmPFC and behavior in humans corresponded to model predictions. Additional experiments (Supplemental Modeling, SI.7,8) showed the value of a third, non-transient, choosable option exerts two kinds of influences on accuracy. As its value increases and approaches that of the best option, inaccuracy increases because it is itself more often chosen, as has been reported before[40]. However, when the third option is much lower in value, inaccuracy increases because more second best choices are made.

In humans, it is not possible to take time-resolved measures of neurotransmitters to test whether lower levels of inhibition occur when distractors have low values as the model predicts. Average vmPFC GABA concentrations, however, can be measured and they are associated with worse average two-option decision-making[28].

It is not possible to describe the impact of the distractor on behavior and vmPFC value difference signals in terms of divisive normalization accounts such as those proposed by Louie and colleagues[27] to describe distractor effects in parietal cortex, even if vmPFC neurons with activity that is positively and negatively related to value are intermingled as has been reported in other frontal lobe regions[41]. Critically, however, when the fMRI data were re-analyzed, a *spatially selective* value signal–a contralateral chosen value signal specific to one response side–was found in MIP and its size was reduced in proportion to the value of alternatives on the other response side (Fig.7b) just as predicted by divisive normalization accounts[27]. Behavioral tasks requiring more spatially resolved responses (reaching movements to four different locations corresponding to the different potential stimulus quadrants) and employing more spatially resolved recording of brain signals might be necessary to identify a normalizing effect of stimuli presented in a different quadrant in the same hemifield as the COpt[27].

Our version of Wang's biophysical model predicts both subjects' choices and vmPFC activity patterns. It is, however, possible that biophysical models of other networks might produce the activity patterns both we and Louie and colleagues[27] observed in parietal cortex[4,42].

That the current biophysical model provided a better description of vmPFC than IPS activity it is unlikely to reflect some vagary of task design. Care was taken to index values with conjunctions of simple visual features known to rely on parietal cortex[43,44]. Similar speeded response requirements were used in monkey experiments that reported parietal value signals[14,15]. Moreover, training of the sort subjects undertook before scanning leads to greater IPS activity during action selection[45]. That we were able to find value signals in MIP attests to the appropriateness of our protocol. Instead, the results suggest fundamental differences between vmPFC and IPS decision-making mechanisms. VmPFC neurons may employ more abstract and flexible coding principles than do spatially selective IPS neurons. Little is known of vmPFC neuron properties but what is known suggests differences from lOFC[2,9-11,31,33,46-48].

We note that previous studies have presented evidence for encoding of the difference in value between options[49] and for value normalization[27] in the intraparietal sulcus. Here we provide some evidence that the human intraparietal region encodes the value difference between options (Fig.3d) but that spatial value signals are normalized in the same brain region even by the values of irrelevant stimuli (Fig.7).

While the nature of the vmPFC decision-making mechanism may cause failure of optimal choice in some circumstances, it has the advantage of favoring "satisficing" choices when time for deliberation is limited[50] –choices that, while not ideal, are likely to be good given the options currently available; this is because failure of optimal choice only occurs when HV and LV are close in value. If time and resources for taking a decision are at a premium, as in many natural settings, then the vmPFC mechanism allows fast satisficing decisions to be made. It leads people to pick the second best option when the best and second best options are close in value and when the best and second options are both much better than another alternative.

Our results resonate with the notion that IPS and vmPFC constitute two components of a system for value-based choice[8] but suggest both components might simultaneously attempt to select the course of behavior. That individual variation in both vmPFC (Fig.5b) and MIP (Fig.7b) signals was correlated with individual variation in two distinct aspects of behavior supports this view. Moreover such a view is consistent with a demonstration that high value distractors, in a non-spatial task, sometimes only disrupted decision-making in the manner divisive normalization accounts predict after vmPFC lesion[2]. This could be explained if, in the absence of vmPFC, the divisive normalization effect of distractors on parietal activity had a greater impact on behavior. Such findings may contribute to a growing understanding of failures of optimal decision-making by suggesting that situational variables that favor either parietal or vmPFC control of behavior may determine patterns of deviation away from optimal decision-making.

Online Methods

Biophysical model

The biophysical model is the full spiking network model developed by Wang[24] and subsequently used to investigate reward-guided decision making in both its full spiking form[42] and its reduced mean-field form[51]. The parameters used were mostly the same as in the implementation of the model reported in Wang et al.[24] The only modifications made to account for differences in our task were that we: 1) split the overall number or option specific excitatory pyramidal neuronal pools into three equal populations, each containing 240 neurons; 2) only gave value input to the “distractor” option for the first 100ms after stimulus onset (corresponding to the time period before revelation of distractor identity in subsequent experiments, whereas the value inputs of the two available options were given for a total of 800ms. The scaling of the value-related input was selected at 17.5 arbitrary units with a variance of 25 arbitrary units to match the average relationship between value difference and accuracy in human subjects (Fig.1b). Timings of stimulus onset, distractor removal and increased noise can be seen in figure 1c/d. The model simulation contained 149 trials of different option value combinations. We repeated the model 36 times (i.e. 5364 trials in total) and pooled results for our statistical analyses. The firing time courses shown were generated from the original time courses by averaging firing from 10 samples per millisecond to one sample every 10 milliseconds.

We focus on examining activity and inhibition in neuron pools corresponding to available options (Fig.1c-f). In addition, however, we also generated model “choices” once P_{HV} and P_{LV} had a firing difference of 6 Hz (Fig.1g).

Subjects

Twenty one healthy, right-handed subjects (nine females), aged 19-34 years with no psychiatric or neurological history participated. Informed consent was obtained from every subject. The study was approved by the Oxfordshire National Health Service Research Ethics Committee.

Experimental task

In our fMRI task, subjects chose repeatedly between stimuli associated with different reward magnitudes (£2, £4, £6, £8, £10, £12) and probabilities (12.5%, 25%. 37.5%, 50%, 62.5%, 75%, 87.5%), represented by colors (red to blue) and orientations (0° to 90°) of rectangular bars. Associations between visual features and decision variables were counterbalanced across subjects. Participants were presented with 150 trials each of two-option trials and distractor trials (300 trials in total) randomly interleaved. All the option value configurations in the distractor trials were identical to those used in the biophysical model; those in the two-option trials were also matched with the *available* options in the distractor trials. Each trial began with a central fixation cross indicating an inter-trial interval (3-6 s) followed by an *initial phase* in which two (two-option trials) or three (distractor trials) stimuli were presented in randomly selected screen quadrants. The initial phase was brief – only 0.1 s. Then, in the *decision phase*, orange boxes were presented around two stimuli indicating those options were available for choice. In distractor trials, a purple box was also presented around the third stimulus to indicate a distractor. Subjects were instructed to select one of the available options within 1.5 s. Subjects were warned they were “too slow” if no response was made within 1.5 s and a new trial began. After an option was chosen, the box surrounding it turned red in the *interval phase* (1-3 s). Then the edge of each stimulus turned yellow or grey in the *outcome phase* to indicate, respectively, whether the choice had been rewarded or not (1-3 s). The final reward allocated to the subject on leaving the experiment was calculated by averaging the outcome of all trials. Subjects learned the task and visual feature associations and experienced Distractor trials in a practice session before scanning. At the end of practice, all subjects chose HV on >70% of two-option trials when it was associated with both higher reward magnitude and probability.

We provided incentives for subjects to attend to the visual features of every stimulus by interleaving “catch” trials between decision phase and interval phase in 15% of all the trials. In this way we ensured that it was unlikely that subjects would ignore the distractor values. In a “catch” trial, the word “MATCH” was presented once subjects selected an option in the decision phase (1 s). Then, an exemplar stimulus was presented at the center of the screen and subjects had to indicate, within 2 s, the position of the same stimulus presented before and during the decision phase. Feedback was then given to indicate whether the response was correct or not (1.5 s). The trial then continued with the resumption of the interval phase, followed by the outcome phase. Each correct response in the “catch” trial added an extra 10 pence to the final reward.

Behavioral and biophysical model analysis

The value of each option was calculated by multiplying the associated reward magnitude and probability. The difference in value between the available options and the distractor can be indexed in various ways, HV−D, LV-D, or (average of (HV and LV)-D), all of which are correlated (a consequence of keeping the correlations between HV−LV, HV−D, and D low), and essentially similar results follow in all cases. Here, we report results using HV−D as this might be thought the strongest test of our hypothesis; HV−D is clearly a value difference that is similar in formulation to HV−LV but it should be irrelevant for decision-making. It

would therefore be especially striking if HV−D influenced the impact HV−LV had on behavior and brain activity (figure 5 illustrates a situation where this is true).

A logistic regression was performed for every subject to predict accuracy with the following regressors: value difference between higher and lower value options (HV−LV), value difference between available option and distractor (HV−D), (HV−LV)(HV−D) interaction, HV+LV and a binary variable describing trial type. Alternative regression analyses are also presented (SI.5).

The β weight of each regressor of every subject was calculated and then a one-sample t-test against zero was computed. Such a test identified regressor effects that replicated throughout the group of participants. Two dimensional plots (Fig.2c) were generated to illustrate behavioral effects by binning each distractor trial according to HV−LV and HV−D. General linear models (GLMs) with similar regressors were used in biophysical model analyses.

To examine divisive normalization effects on behavior, we performed another logistic regression that included values of chosen option (COpt), ipsilateral options (IV), the interaction COptxIV, value of unchosen option or distractor when they were on the same side as COpt and its interaction with COpt to predict reaction time (RT).

Imaging data acquisition and preprocessing

Imaging data were acquired on a Siemens 3T MRI scanner. FMRI data were acquired with 3×3×3 mm^3 voxel-resolution, TR=3 s, TE=30 ms, flip angle=87°, slice angle =15°. Signal dropout in vmPFC was minimized by applying z-shimming at this region[52]. Field maps were acquired using a dual echo 2D gradient echo sequence: 3×3×3 mm^3 voxel-resolution, TR=445 ms, TE 1=5.19 ms, TE 2=7.65 ms. T1-weighted structural images were acquired using an MPRAGE sequence: 1×1×1 mm^3 voxel-resolution, 174×192×192 grid, TR=2200 ms, TE=4.53 ms, TI=900 ms.

FMRI data were analyzed using FMRIB's Software Library (FSL)[53]. Preprocessing was performed by applying high-pass temporal filtering (3 dB cutoff of 100 s), Gaussian spatial smoothing (full-width half maximum of 5 mm), motion correction[54] and field map correction for signal distortion[55]. Motion artefact was removed by performing independent component analysis using FSL MELODIC. Each individual's fMRI data set was registered to the same individual's high-resolution structural image and then into the standard Montreal Neurological Institute (MNI) space using affine transformations[56].

FMRI data analysis

Whole-brain analyses were conducted using a univariate GLM approach. At the group level, analyses were performed using FMRIB's local analysis of mixed effects[57,58], with outlier deweighting[59] and cluster-based thresholding criteria of $z>2.3$ and $p<.05$ cluster-corrected[60], unless otherwise specified.

To identify brain regions encoding value difference, we included the following regressors: chosen-unchosen value difference in two-option trials, chosen-unchosen value difference in distractor trials, and HV−D in distractor trials, time-locked to stimulus onset; left hand

response, right hand response, time-locked to subjects' response; magnitude of reward feedback and feedback indicating inappropriate responses (mistakenly choosing a blank space or distractor) and slow responses, time-locked to feedback onset; and feedback on catch trials time-locked to its onset.

We extracted MIP and vmPFC signals from three-voxel radius spherical masks at coordinates from our previous studies of MIP[25] and vmPFC[5,18] (which corresponded to the peak effect in the current study). Coordinates in MNI space were transformed to subject space by affine transformation. The extracted time courses were 10 times oversampled by cubic spline interpolation. The time courses were then time-locked to onset of the initial phase and were analyzed by applying a GLM to every time point of each subject separately. The mean and standard error of the β weights of regressors were calculated across subjects so that time courses of effect sizes could be plotted. To illustrate the value difference signals in vmPFC and MIP we analyzed the distractor trials by including regressors of HV−LV, HV −D, HV+LV and magnitude of reward feedback in the GLM (Fig.3c,3d). In Fig.5a we also included an additional (HV−LV)(HV−D) interaction term regressor. Note that because we focused on correct trials only, the HV−LV signal that corresponds to the chosen-unchosen value signal previously reported in vmPFC. In Fig.7a, we looked at modulation of the MIP COpt signal. The following regressors were included in the GLM: COpt, IV, and the interaction between these two regressors COpt×IV (which served as our critical measure of modulation), magnitude of reward feedback, and a binary variable describing trial type. Error bars in all the figures represent standard error.

To investigate modulation of the HV−LV value difference signal by distractor (Fig.4a,b), we separated the distractor trials into four bins according to HV−D difference (>150, 0 to 150, −150 to 0, <−150). Four corresponding bins were identified in the two-option trials. The matched trials were, by design, identical to distractor trials in terms of available options (HV and LV) but obviously they lacked a distractor. We included in our analysis for a given participant only matched pairs of trials when correct responses were made in both trials. It is important to use only correct trials in the analysis because the vmPFC decision signal reflects the chosen-unchosen option value difference and this would differ between correctly and incorrectly performed versions of the same trial. We applied a GLM to each bin of every subject that included regressors of the HV−LV value difference and the magnitude of reward feedback. The peak HV−LV value difference signal in each bin was extracted in every subject within a 5-11 s time window from onset of the initial phase. Linear regression was performed to predict HV−LV signal size by the HV−D value difference rank associated with the four bins for each trial type. The β weight for HV−D rank was an index of modulation in HV−LV signal size by HV−D. A two-tailed one sample t-test compared the group's β weights with zero to determine consistency and significance of modulation.

A similar analysis was performed to investigate the divisive normalization effect on the COpt signal. We took correct trials where choices were made with the hand contralateral to the ROI and binned them according to IV. Effect sizes in each bin were derived from a GLM with a regressor of COpt. The maximum COpt signal of each subject was extracted from a time window where group effects peaked (MIP, 12-18 s; vmPFC, 5-11 s).

We performed partial correlations to examine relationships between neural signals and different aspects of behavior. We extracted the effect size of the impact of HV−D on the HV −LV signal (Fig.5a), as indexed by the maximum (HV−LV)(Op-D) signal (13-19 s), from every subject and correlated it with the subjects' accuracies in distractor trials. The control variables were sizes of HV−LV and HV−D signals and RT in distractor trials. In Fig.5c, we subtracted the maximum (HV−LV)(HV−D) signal in a 13-19 s time window from that in a 2-7 s time window to obtain the size of signal reduction and correlated this with subjects' distractor trials accuracies. A second analogous analysis in the divisive normalization analysis (Fig.7b) examined partial correlation between each subject's maximum effect size for the interaction term COptxIV (12-18 s) and mean RT. Control variables were sizes of COpt and IV signals and accuracy.

Psychophysiological interaction analysis

We performed a psychophysiological interaction (PPI) analysis[61] to examine how vmPFC coupled with other brain regions to encode HV−LV and HV−D value differences. Each PPI regressor was generated by multiplying the demeaned physiological regressor (time course of vmPFC BOLD) by the demeaned, convolved psychological regressor (either HV−LV or HV−D value differences in distractor trials). We entered the following regressors into the GLM: time course of vmPFC, HV−LV value difference in distractor trials and its PPI with vmPFC, HV−D value difference in distractor trials and its PPI with vmPFC, HV−LV value difference in two-option trials, left hand response, right hand response, number of stimuli presented, magnitude of reward feedback, feedback on the catch trials and feedbacks indicating inappropriate and slow responses. We initially used a cluster-based threshold ($z > 2.3$, $p<.05$ Fig.6a) and then a more stringent cluster-based thresholding criterion of $z > 2.7$, $p<.05$ (Fig.6b) to reduce the possibility of any false positive results in follow-up analysis.

Supplementary Material

Refer to Web version on PubMed Central for supplementary material.

References

1. Vickery TJ, Chun MM, Lee D. Ubiquity and Specificity of Reinforcement Signals throughout the Human Brain. Neuron. 2011; 72:166–177. [PubMed: 21982377]
2. Noonan MP, et al. Separate value comparison and learning mechanisms in macaque medial and lateral orbitofrontal cortex. Proc Natl Acad Sci U S A. 2010; 107:20547–20552. [PubMed: 21059901]
3. Hunt LT, et al. Mechanisms underlying cortical activity during value-guided choice. Nat Neurosci. 2012
4. Wang XJ. Neural dynamics and circuit mechanisms of decision-making. Curr Opin Neurobiol. 2012; 22:1039–1046. [PubMed: 23026743]
5. Boorman ED, Behrens TE, Woolrich MW, Rushworth MF. How green is the grass on the other side? Frontopolar cortex and the evidence in favor of alternative courses of action. Neuron. 2009; 62:733–743. [PubMed: 19524531]
6. Camille N, Griffiths CA, Vo K, Fellows LK, Kable JW. Ventromedial frontal lobe damage disrupts value maximization in humans. J Neurosci. 2011; 31:7527–7532. [PubMed: 21593337]
7. Rangel A, Camerer C, Montague PR. A framework for studying the neurobiology of value-based decision making. Nat Rev Neurosci. 2008; 9:545–556. [PubMed: 18545266]

8. Kable JW, Glimcher PW. The neurobiology of decision: consensus and controversy. Neuron. 2009; 63:733–745. [PubMed: 19778504]
9. Rushworth MF, Noonan MP, Boorman ED, Walton ME, Behrens TE. Frontal cortex and reward-guided learning and decision-making. Neuron. 2011; 70:1054–1069. [PubMed: 21689594]
10. Bouret S, Richmond BJ. Ventromedial and orbital prefrontal neurons differentially encode internally and externally driven motivational values in monkeys. J Neurosci. 2010; 30:8591–8601. [PubMed: 20573905]
11. Monosov IE, Hikosaka O. Regionally distinct processing of rewards and punishments by the primate ventromedial prefrontal cortex. J Neurosci. 2012; 32:10318–10330. [PubMed: 22836265]
12. Lebreton M, Jorge S, Michel V, Thirion B, Pessiglione M. An automatic valuation system in the human brain: evidence from functional neuroimaging. Neuron. 2009; 64:431–439. [PubMed: 19914190]
13. Kable JW, Glimcher PW. The neural correlates of subjective value during intertemporal choice. Nat Neurosci. 2007; 10:1625–1633. [PubMed: 17982449]
14. Platt ML, Glimcher PW. Neural correlates of decision variables in parietal cortex. Nature. 1999; 400:233–238. [PubMed: 10421364]
15. Louie K, Glimcher PW. Separating value from choice: delay discounting activity in the lateral intraparietal area. J Neurosci. 2010; 30:5498–5507. [PubMed: 20410103]
16. FitzGerald TH, Seymour B, Dolan RJ. The role of human orbitofrontal cortex in value comparison for incommensurable objects. J Neurosci. 2009; 29:8388–8395. [PubMed: 19571129]
17. Philiastides MG, Biele G, Heekeren HR. A mechanistic account of value computation in the human brain. Proc Natl Acad Sci U S A. 2010; 107:9430–9435. [PubMed: 20439711]
18. Kolling N, Behrens TE, Mars RB, Rushworth MF. Neural mechanisms of foraging. Science. 2012; 336:95–98. [PubMed: 22491854]
19. De Martino B, Fleming SM, Garrett N, Dolan RJ. Confidence in value-based choice. Nat Neurosci. 2013; 16:105–110. [PubMed: 23222911]
20. Hare TA, Schultz W, Camerer CF, O'Doherty JP, Rangel A. Transformation of stimulus value signals into motor commands during simple choice. Proc Natl Acad Sci U S A. 2011; 108:18120–18125. [PubMed: 22006321]
21. Summerfield C, Tsetsos K. Building Bridges between Perceptual and Economic Decision-Making: Neural and Computational Mechanisms. Frontiers in neuroscience. 2012; 6:70. [PubMed: 22654730]
22. Churchland AK, Kiani R, Shadlen MN. Decision-making with multiple alternatives. Nat Neurosci. 2008; 11:693–702. [PubMed: 18488024]
23. Usher M, McClelland JL. The time course of perceptual choice: the leaky, competing accumulator model. Psychological review. 2001; 108:550–592. [PubMed: 11488378]
24. Wang XJ. Probabilistic decision making by slow reverberation in cortical circuits. Neuron. 2002; 36:955–968. [PubMed: 12467598]
25. Mars RB, et al. Diffusion-weighted imaging tractography-based parcellation of the human parietal cortex and comparison with human and macaque resting-state functional connectivity. J Neurosci. 2011; 31:4087–4100. [PubMed: 21411650]
26. Gould IC, Nobre AC, Wyart V, Rushworth MF. Effects of decision variables and intraparietal stimulation on sensorimotor oscillatory activity in the human brain. J Neurosci. 2012; 32:13805–13818. [PubMed: 23035092]
27. Louie K, Grattan LE, Glimcher PW. Reward value-based gain control: divisive normalization in parietal cortex. J Neurosci. 2011; 31:10627–10639. [PubMed: 21775606]
28. Jocham G, Hunt LT, Near J, Behrens TE. A mechanism for value-guided choice based on the excitation-inhibition balance in prefrontal cortex. Nat Neurosci. 2012; 15:960–961. [PubMed: 22706268]
29. Wunderlich K, Dayan P, Dolan RJ. Mapping value based planning and extensively trained choice in the human brain. Nat Neurosci. 2012; 15:786–791. [PubMed: 22406551]

30. Lim SL, O'Doherty JP, Rangel A. The Decision Value Computations in the vmPFC and Striatum Use a Relative Value Code That is Guided by Visual Attention. J Neurosci. 2011; 31:13214–13223. [PubMed: 21917804]
31. Rudebeck PH, Murray EA. Dissociable effects of subtotal lesions within the macaque orbital prefrontal cortex on reward-guided behavior. J Neurosci. 2011; 31:10569–10578. [PubMed: 21775601]
32. Walton ME, Behrens TE, Buckley MJ, Rudebeck PH, Rushworth MF. Separable learning systems in the macaque brain and the role of orbitofrontal cortex in contingent learning. Neuron. 2010; 65:927–939. [PubMed: 20346766]
33. Noonan MP, Mars RB, Rushworth MF. Distinct Roles of Three Frontal Cortical Areas in Reward-Guided Behavior. Journal of Neuroscience. 2011
34. Fellows LK. Deciding how to decide: ventromedial frontal lobe damage affects information acquisition in multi-attribute decision making. Brain. 2006; 129:944–952. [PubMed: 16455794]
35. Lee J, Maunsell JH. A normalization model of attentional modulation of single unit responses. PLoS One. 2009; 4:e4651. [PubMed: 19247494]
36. Lee J, Maunsell JH. Attentional modulation of MT neurons with single or multiple stimuli in their receptive fields. J Neurosci. 2010; 30:3058–3066. [PubMed: 20181602]
37. Sugrue LP, Corrado GS, Newsome WT. Choosing the greater of two goods: neural currencies for valuation and decision making. Nat Rev Neurosci. 2005; 6:363–375. [PubMed: 15832198]
38. Padoa-Schioppa C. Range-adapting representation of economic value in the orbitofrontal cortex. J Neurosci. 2009; 29:14004–14014. [PubMed: 19890010]
39. Palminteri S, Boraud T, Lafargue G, Dubois B, Pessiglione M. Brain hemispheres selectively track the expected value of contralateral options. J Neurosci. 2009; 29:13465–13472. [PubMed: 19864559]
40. Louie K, Khaw MW, Glimcher PW. Normalization is a general neural mechanism for context-dependent decision making. Proceedings of the National Academy of Sciences. 2013
41. Wallis JD, Kennerley SW. Heterogeneous reward signals in prefrontal cortex. Curr Opin Neurobiol. 2010; 20:191–198. [PubMed: 20303739]
42. Soltani A, Wang XJ. A biophysically based neural model of matching law behavior: melioration by stochastic synapses. J Neurosci. 2006; 26:3731–3744. [PubMed: 16597727]
43. Ashbridge E, Walsh V, Cowey A. Temporal aspects of visual search studied by transcranial magnetic stimulation. Neuropsychologia. 1997; 35:1121–1131. [PubMed: 9256377]
44. Sereno AB, Maunsell JHR. Shape selectivity in primate lateral intraparietal cortex. Nature. 1998; 395:500–502. [PubMed: 9774105]
45. Grol MJ, de Lange FP, Verstraten FA, Passingham RE, Toni I. Cerebral changes during performance of overlearned arbitrary visuomotor associations. J Neurosci. 2006; 26:117–125. [PubMed: 16399678]
46. Noonan MP, Kolling N, Walton ME, Rushworth MF. Re-evaluating the role of the orbitofrontal cortex in reward and reinforcement. Eur J Neurosci. 2012; 35:997–1010. [PubMed: 22487031]
47. Wallis JD. Cross-species studies of orbitofrontal cortex and value-based decision-making. Nat Neurosci. 2012; 15:13–19. [PubMed: 22101646]
48. Kaping D, Vinck M, Hutchison RM, Everling S, Womelsdorf T. Specific contributions of ventromedial, anterior cingulate, and lateral prefrontal cortex for attentional selection and stimulus valuation. PLoS Biol. 2011; 9:e1001224. [PubMed: 22215982]
49. Seo H, Barraclough DJ, Lee D. Lateral intraparietal cortex and reinforcement learning during a mixed-strategy game. J Neurosci. 2009; 29:7278–7289. [PubMed: 19494150]
50. Simon HA. Rational choice and the structure of the environment. Psychological Review. 1956; 63:129–138. [PubMed: 13310708]
51. Hunt LT, et al. Mechanisms underlying cortical activity during value-guided choice. Nat Neurosci. 2012; 15:470–476. S471–473. [PubMed: 22231429]
52. Deichmann R, Gottfried JA, Hutton C, Turner R. Optimized EPI for fMRI studies of the orbitofrontal cortex. Neuroimage. 2003; 19:430–441. [PubMed: 12814592]

53. Smith SM, et al. Advances in functional and structural MR image analysis and implementation as FSL. Neuroimage. 2004; 23(Suppl 1):S208–219. [PubMed: 15501092]

54. Jenkinson M, Bannister P, Brady M, Smith S. Improved optimization for the robust and accurate linear registration and motion correction of brain images. Neuroimage. 2002; 17:825–841. [PubMed: 12377157]

55. Jenkinson M. Fast, automated, N-dimensional phase-unwrapping algorithm. Magnetic resonance in medicine : official journal of the Society of Magnetic Resonance in Medicine / Society of Magnetic Resonance in Medicine. 2003; 49:193–197.

56. Jenkinson M, Smith S. A global optimisation method for robust affine registration of brain images. Medical image analysis. 2001; 5:143–156. [PubMed: 11516708]

57. Beckmann CF, Jenkinson M, Smith SM. General multilevel linear modeling for group analysis in FMRI. Neuroimage. 2003; 20:1052–1063. [PubMed: 14568475]

58. Woolrich MW, Behrens TE, Beckmann CF, Jenkinson M, Smith SM. Multilevel linear modelling for FMRI group analysis using Bayesian inference. Neuroimage. 2004; 21:1732–1747. [PubMed: 15050594]

59. Woolrich M. Robust group analysis using outlier inference. Neuroimage. 2008; 41:286–301. [PubMed: 18407525]

60. Worsley KJ, Evans AC, Marrett S, Neelin P. A three-dimensional statistical analysis for CBF activation studies in human brain. J Cereb Blood Flow Metab. 1992; 12:900–918. [PubMed: 1400644]

61. Friston KJ, et al. Psychophysiological and modulatory interactions in neuroimaging. Neuroimage. 1997; 6:218–229. [PubMed: 9344826]

Europe PMC Funders Author Manuscripts

Europe PMC Funders Author Manuscripts

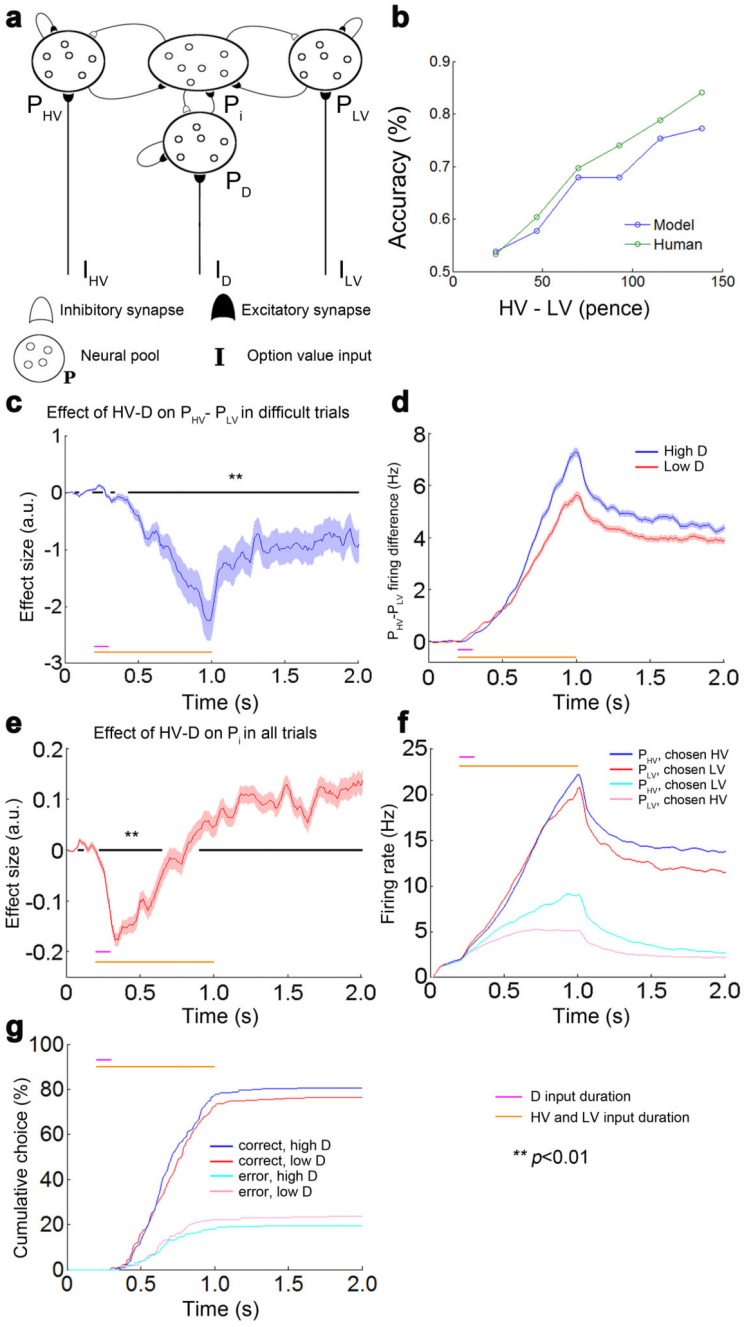

Figure 1.

Biophysical model predictions. **(a)** The biophysical model is similar to models used elsewhere[3,24] but extended to contain three pools of excitatory pyramidal neurons (P_{HV}, P_{LV}, P_D) corresponding to choices of either the high value or low value available option or the distractor D. There is recurrent excitation between neurons within pools but inhibitory interneurons (P_i) mediate competition between pools. Activity in each pool is initially affected by an input proportional (I_{Hv}, I_{LV}, I_D) to the value of each option (I_{HV} and I_{LV} was on between 200-1000 ms and I_D was on between 200 and 300 ms) but inhibition between

pools leaves only a single pool in a high firing attractor state. The corresponding option is then chosen. **(b)** The scaling of the value related input was selected at 17.5 arbitrary units with a variance of 25 arbitrary units so as to match the average relationship found between value difference and accuracy seen in the human subjects tested in the subsequent behavioral experiment (Fig.2). The model's "choices" were defined once P_{HV} and P_{LV} had a firing difference of 6 Hz. **(c)** The magnitude of difference in the activity of P_{HV} and P_{LV}, which corresponds to the value difference signal (HV−LV) used in fMRI analyses, decreased as a function of increasing size of the irrelevant difference between the available options and the distractor (HV−D) in a regression analysis. The effect for trials when HV−LV was small is shown but a similar analysis performed for all trials is shown in SI.1. **(d)** To see how the effect emerges, average P_{HV} and P_{LV} firing activity at two different levels of D are also shown. **(e)** The effect arises because the amount of inhibitory activity (P_i) increased as HV −D decreased (larger relative distractor value) and P_D inhibited representations of the other two options, P_{HV} and P_{LV} more. In those cases, the competition between P_{HV} and P_{LV} was resolved more quickly, causing a smaller overall input to the inhibitory neurons. **(f)** The excitatory population reached a high attractor state when the corresponding option was chosen by the model. **(g)** When D was much lower in value than the choosable options the model was more likely to make the wrong choice; P_{HV} became less likely to enter the higher firing attractor model state. The shadings (c-e) denote standard error. ** $p<0.01$.

Europe PMC Funders Author Manuscripts

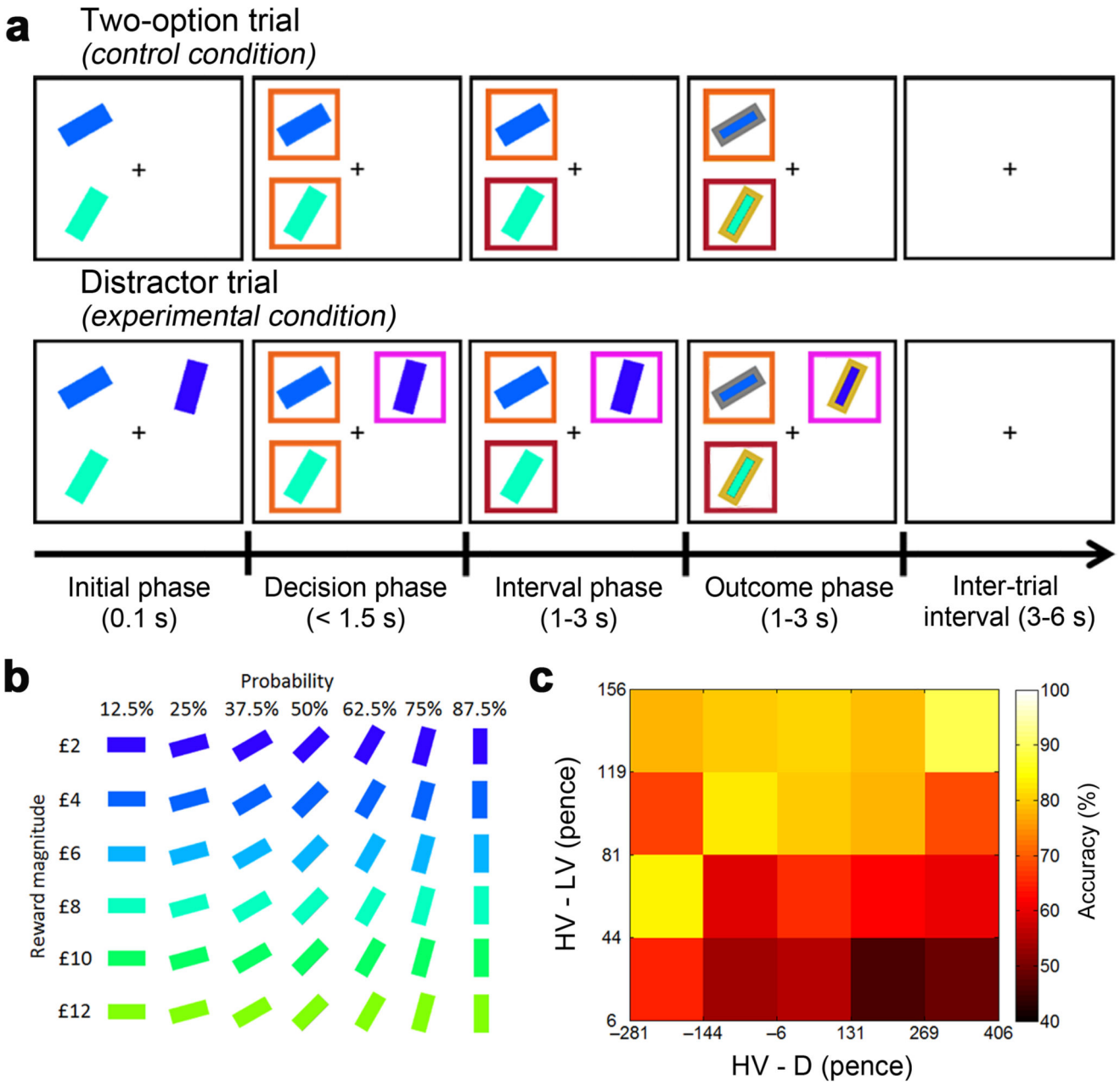

Figure 2.

Behavioral task and results. **(a)** In the initial phase of two-option trials subjects saw two visual stimuli indicating two possible choices. These were immediately surrounded by orange squares, indicating that either option might be chosen, in the decision phase. A further color change during the interval phase of one box indicated which choice the subject made. In the outcome phase of the trial the outline color of the chosen stimulus indicated to the subject whether the reward had been won. The final reward allocated to the subject on leaving the experiment was calculated by averaging the outcome of all trials. Distractor trials unfolded in a similar way but, in the decision phase, one stimulus, the distractor, was

surrounded by a purple square to indicate that it could not be chosen while the presentation of orange squares around the other options indicated that they were available to choose. **(b)** Prior to fMRI scanning subjects learned that stimulus orientation and color indicated the probability and magnitude of rewards if the stimulus was chosen by making a spatially congruent response. In this way choice values were conveyed to the subjects in a simple manner just as they are in macaque experiments on value-coding in parietal cortex **(c)** Choice accuracy (% HV choice) is indicated by color as a function of both the difference in value between the two available options (HV−LV) and the difference in value between available options and the distractor (HV−D). Choices are less accurate when the HV−LV difference is small (bottom of figure contains more red and dark colors than the top) but also, importantly, when HV−D was large (more red and dark colors at the right hand side than the left hand side of the figure) especially when HV−LV was small.

Europe PMC Funders Author Manuscripts

Europe PMC Funders Author Manuscripts

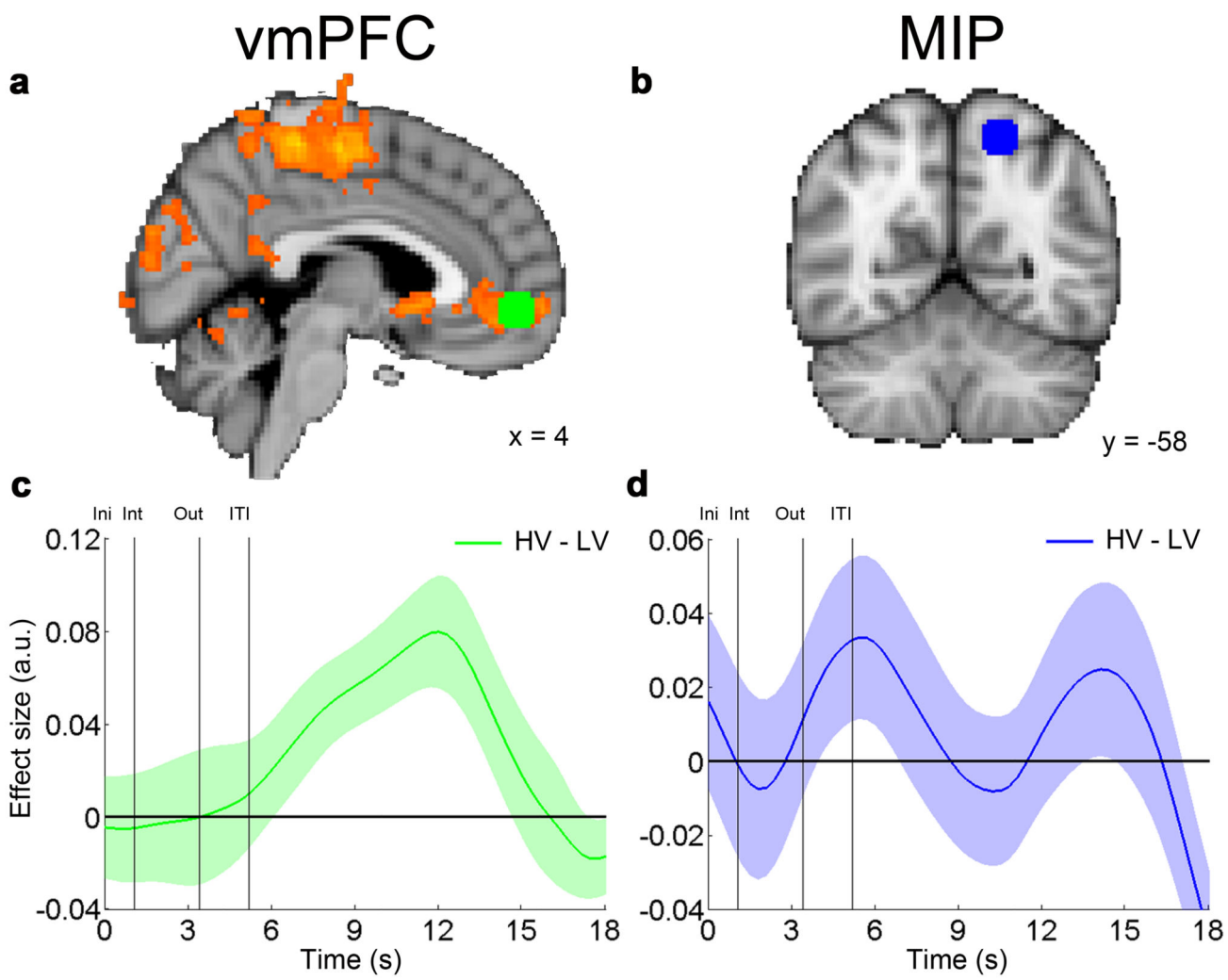

Figure 3.

(a) As in previous experiments there was a prominent value difference effect between available options in vmPFC (sagittal section). An ROI in this region (green) was defined for the subsequent time course analyzes. **(b)** ROI in MIP (blue) with coordinates taken from Mars et al.[25] (coronal section). **(c)** Time course of HV−LV value difference signal in correct trials in vmPFC and **(d)** MIP. Ini, initial phase; Int, interval phase; Out, outcome phase; ITI, inter-trial interval.

Europe PMC Funders Author Manuscripts

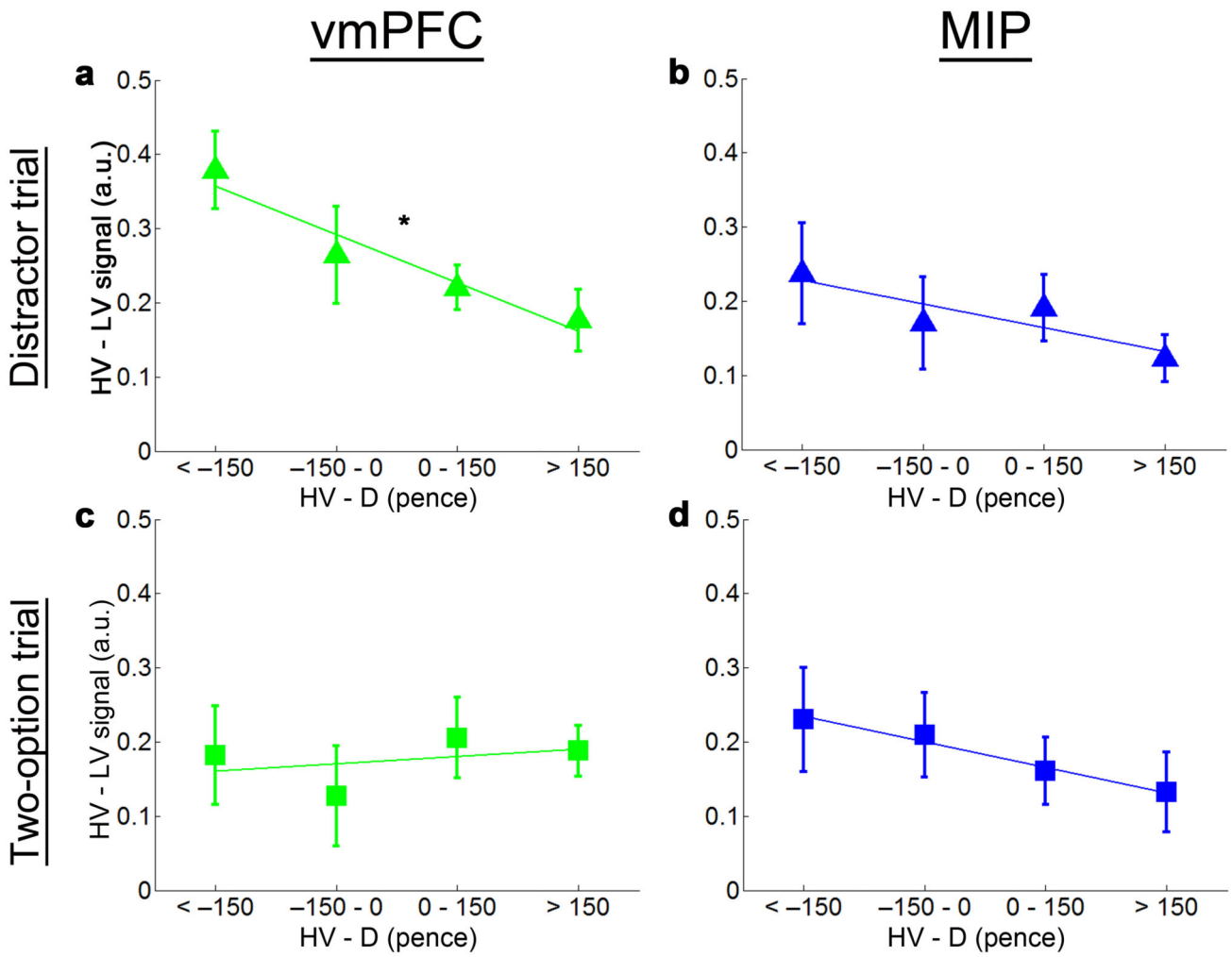

Figure 4.

(a) When the HV−LV value difference signal was binned as a function of the difference in value between available options and the distractor (HV−D) it was clear that, in vmPFC, it declined significantly as HV−D increased (in other words as D was lower) in distractor trials **(c)** but not in matched two-option trials. **(b,d)** No modulation, however, was seen in MIP in either distractor trials or matched Two-option trials.

Error bars in s.e.m.

* Effect size of the slope, p=0.005

Europe PMC Funders Author Manuscripts

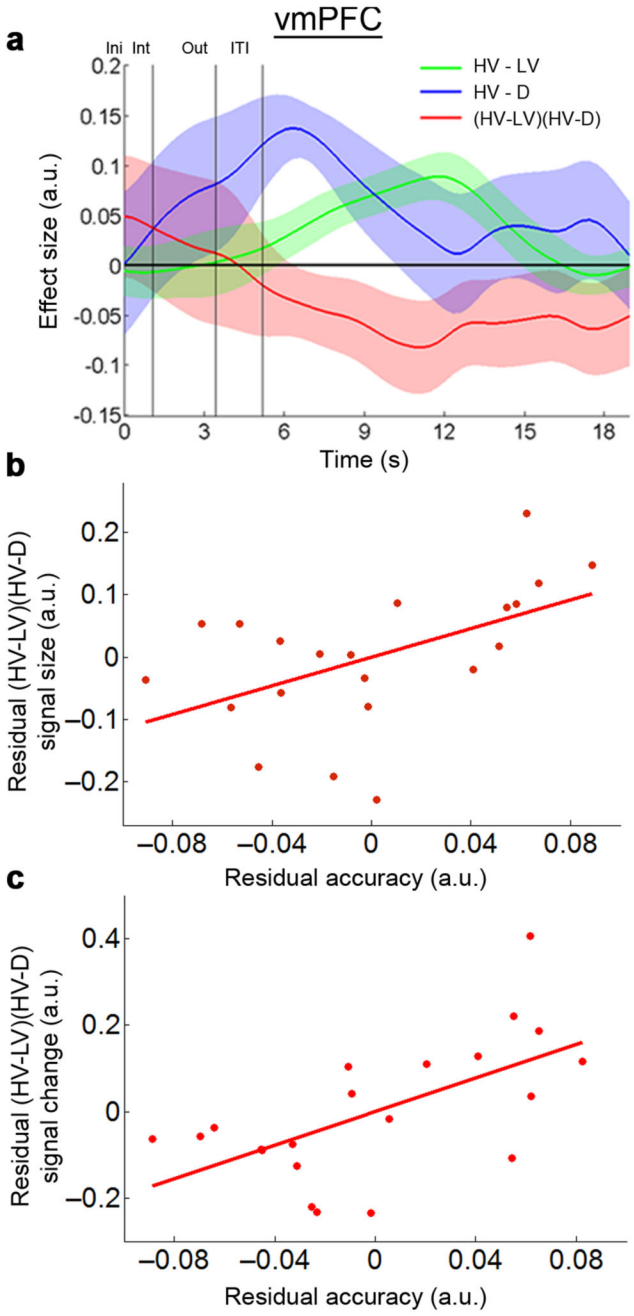

Figure 5.

(a) The distractor-induced modulation of vmPFC HV−LV signals can be seen by a complementary analysis that included regressors corresponding to both the value difference between available options (HV−LV) and to the value difference between available options and the distractor (HV−D) and their interaction (HV−LV)(HV−D). **(b)** Individuals with more negative (HV−LV)(HV−D) interaction signals, especially in a late 13-19 s time window, were associated with less accurate decisions, after controlling for the effects of HV −LV, HV−D signals and RT. **(c)** It appeared that failure to reduce the size of the impact of

the (HV−LV)(HV−D) interaction term on vmPFC BOLD activity was associated with inaccurate choice; individuals with less reduction of the negative (HV−LV)(HV−D) signal in this late time window compared to an earlier 3-7 s time window were more inaccurate.

Europe PMC Funders Author Manuscripts

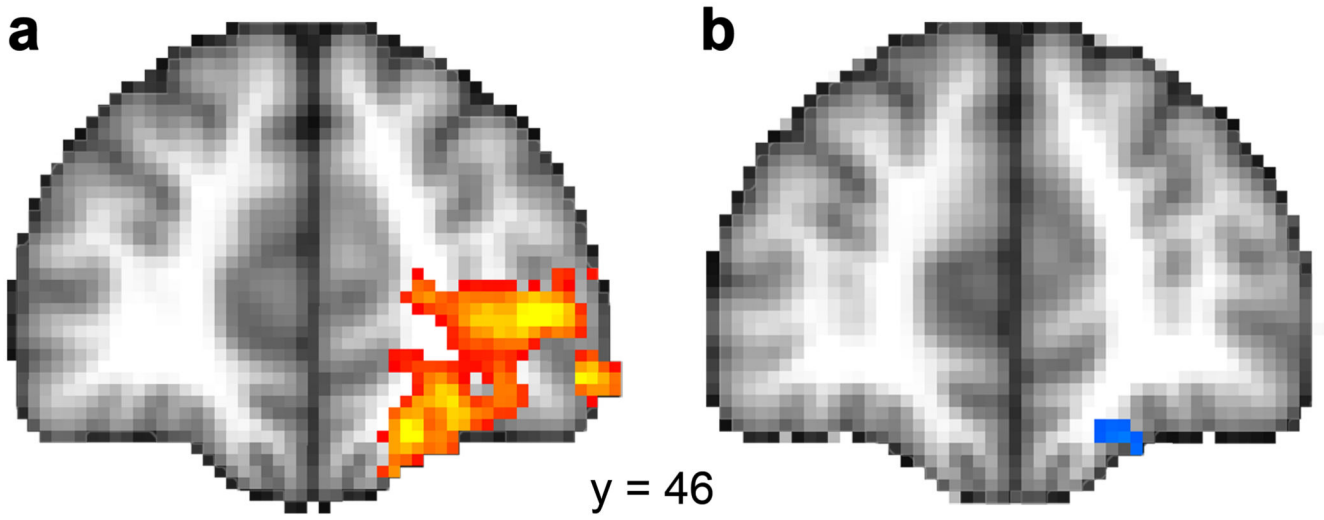

Figure 6.

Psychophysiological Interaction (PPI) results. **(a)** Coupling with vmPFC as a function of the negative effect of the irrelevant comparison between available options and the distractor (HV−D) increased in lateral orbitofrontal and ventrolateral frontal cortex. Representations associated with the irrelevant comparison HV−D were reduced in tandem with vmPFC activity in these regions that are important for representation of individual stimuli and their associated outcomes. **(b)** Coupling with vmPFC as a function of the positive effect of the decision-relevant value difference (HV−LV) increased in part of the same region.

Europe PMC Funders Author Manuscripts

Europe PMC Funders Author Manuscripts

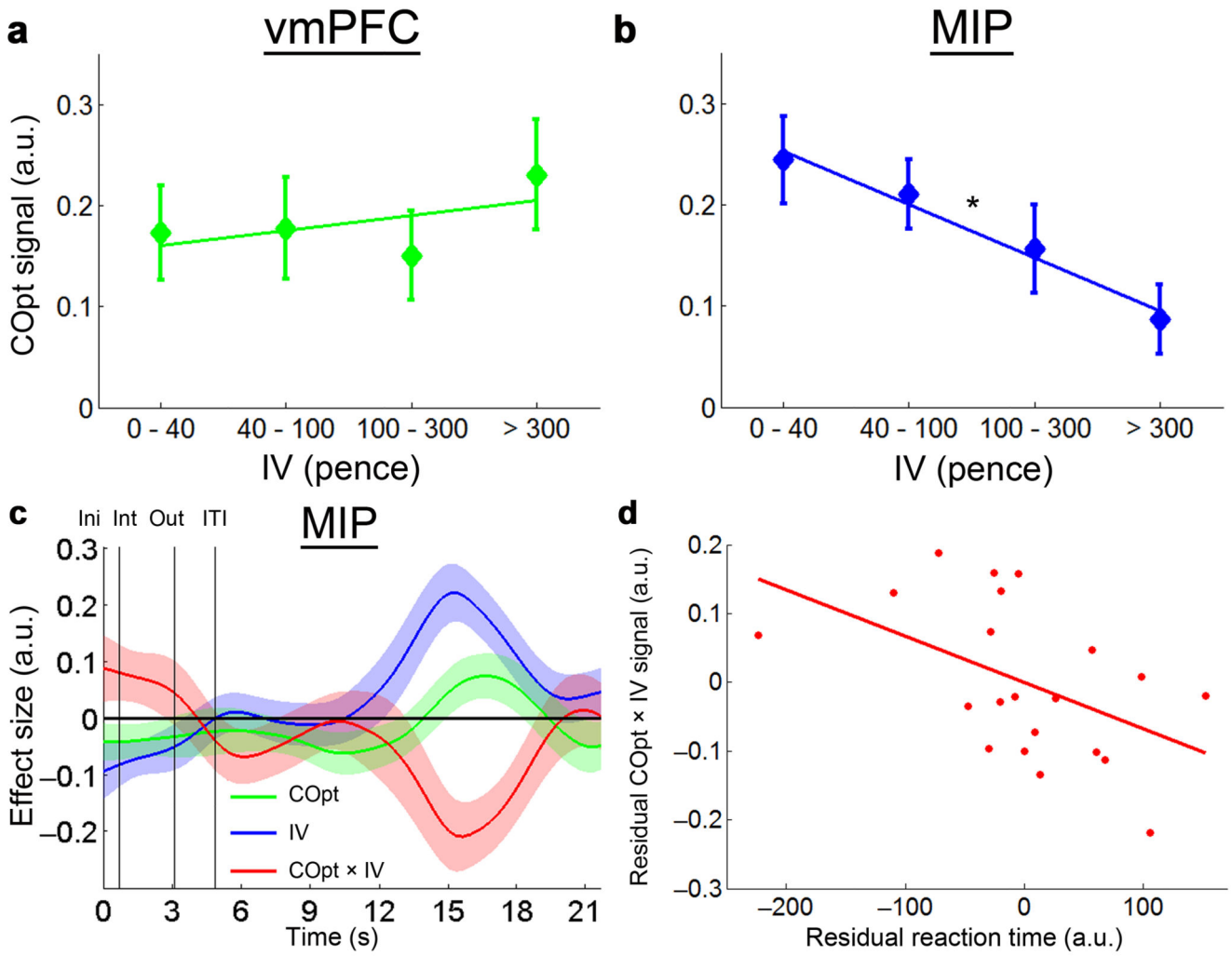

Figure 7.

Divisive normalization of spatially specific contralateral option (COpt) choice signals in MIP. Value signals specific to contralateral responses in vmPFC **(a)** and MIP **(b)**. The value signal decreased as the total value of stimuli (ipsilateral value: IV) associated with the other, ipsilateral, response increased in MIP **(b)** but not vmPFC **(a)**. **(c)** A complementary analysis of the divisive normalization effect of IV on COpt signal in MIP. There was a negative effect of the interaction term COpt×IV suggesting that MIP spatial value signals were diminished in the presence of value associated with the ipsilateral response. **(d)** Individuals with more negative COpt×IV effects had larger average RTs suggesting that greater divisive normalization of spatial value signals in MIP was associated with slower RTs, after controlling for COpt, IV signals and accuracy.

Ini, initial phase; Int, interval phase; Out, outcome phase; ITI, inter-trial interval.

Error bars in s.e.m.

* Effect size of the slope, p=0.003